

Determination of $|V_{cb}|$ from exclusive decays in a relativistic quark model

M. Beyer*

FB Physik Universität Rostock, Universitätsplatz 3, 18051 Rostock, Germany

(Received 17 December 1997; published 15 July 1998)

In the framework of a relativistic covariant Bethe-Salpeter model for the quark-antiquark system we present a renewed determination of the Cabibbo-Kobayashi-Maskawa matrix element $|V_{cb}|$. Complementing an earlier analysis applied to the whole decay spectrum for $B \rightarrow D^* e \nu$ we now also employ the “zero-recoil method” that uses the end point of the decay spectrum ($\omega=1$) and is suited for heavy-to-heavy transitions. The averaged experimental value extracted from the data at zero recoil, $|V_{cb}| \mathcal{F}(\omega=1) = 0.0343 \pm 0.0015$, then leads to $|V_{cb}| = 0.0360 \pm 0.0016$. This value is somewhat larger than the one that uses the whole decay spectrum for the model analysis. We also contrast this result to a nonrelativistic model and to recent experiments on the $B \rightarrow D e \nu$ semileptonic decay. [S0556-2821(98)06515-1]

PACS number(s): 12.15.Hh, 12.39.Ki, 13.20.He, 13.30.Ce

I. INTRODUCTION

Within the standard model the extraction of the Cabibbo-Kobayashi-Maskawa (CKM) matrix element $|V_{cb}|$ (and $|V_{ub}|$) is an outstanding topic of B -meson physics. Several methods have been utilized that are summarized, e.g., by the Particle Data Group [1]. Presently, the value of $|V_{cb}|$ extracted from inclusive decays is somewhat larger than from exclusive decays, e.g., in $B \rightarrow D^* e \nu$.

A fruitful method to extract $|V_{cb}|$ from exclusive decays is to reparametrize the decay data in such a way that they may be fitted by a smooth (e.g., linear) function $|V_{cb}| \mathcal{F}(\omega)$ of ω , where $\omega = (m_B^2 + m_{D^*}^2 - q^2)/(2m_B m_{D^*})$, and q^2 is the four-momentum transfer. Doing so it is possible to extrapolate to the point of zero recoil of the D^* meson, i.e., $\omega = 1$, which is not directly measurable. This procedure is particularly favored in the context of heavy quark effective theory (HQET) [2] but also useful to compare to other approaches since in this context the notion of the whole decay spectrum is not needed to extract $|V_{cb}|$. In HQET the value of \mathcal{F} at zero recoil is normalized up to corrections of order $(\Lambda_{QCD}/m_{c,b})^2$ (where $m_{c,b}$ denotes the mass of the c or b quark). However the required fitting and extrapolation procedure leads to some errors, where the statistical error is under control and presently in the order of 5% [3].

Alternatively, quark models have been proven very useful as they provide not only predictions for $\mathcal{F}(\omega)$ for all ω and $|V_{cb}|$, but also numerous testable results for quite different processes [4–12]. A general overview on bound state models for heavy hadron decay form factors has been given by Ref. [13]. Other approaches the physics of heavy quarks has profited from are QCD sum rules [14] and lattice QCD [15].

Since $\mathcal{F}(\omega)$ is known for a quark model, one may ask for the implications on the empirical value for $|V_{cb}|$, if the zero-recoil result is contrasted to the one obtained by using the whole decay spectrum. Both methods are frequently used but not yet compared to each other directly. In addition, relativistic quark models also allow us to describe heavy-to-light

transitions, in particular $B \rightarrow \pi(\rho)$, important to determine $|V_{ub}|$; see, e.g., Ref. [16]. In this sense the heavy-to-heavy transitions provide an important test case and bear an impression of possible model uncertainties.

In this context the merit of semileptonic $B \rightarrow D^{(*)} e \nu$ transitions may be considered twofold: As already mentioned they provide a very good source to extract the CKM matrix element $|V_{cb}|$ that has to be contrasted to inclusive and non-leptonic decays. On the other hand, weak decays (in general) provide important complementary information for QCD-motivated modeling of the underlying quark structure of mesons (in general, hadrons). In addition, they may be considered useful to discuss the different relativistic approximations used in this context.

We choose an approach utilizing the instantaneous Bethe-Salpeter equation to treat the $q\bar{q}$ system within a relativistically covariant formalism [17]. The model is able to describe the meson mass spectrum for low radial excitations. It has been applied to the calculation of leptonic decays, viz., decay constants and $\gamma\gamma$ decays [18], and to elastic form factors of mesons [19] as well as to charmonium and bottomonium [20]. Relativistic quark models have been investigated, e.g., in Refs. [21–25].

II. BETHE-SALPETER APPROACH

A. Solving the Bethe-Salpeter equation

The Bethe-Salpeter approach provides a consistent treatment of two-body bound states as well as the coupling of an external field via the Mandelstam formalism [26,27]. In order to actually solve the bound state problem several reasonable approximations are necessary or practical: (i) The quark propagators are assumed to be free propagators irrespective of the confinement that is introduced via a confining kernel, (ii) quark masses are assumed to be constant (i.e., constituent quark mass) which is reasonable for heavy quarks, since current quark masses and constituent quark masses needed for reproducing the mesonic mass spectrum are rather close to each other, (iii) we utilize a ladder approximation for the interaction kernel, and (iv) using an instantaneous interaction in addition leads to computational advantages, as it provides

*Email address: beyer@darss.mpg.uni-rostock.de

random-phase-approximation- (RPA-) type equations [28] that can be solved by introducing an effective Hamiltonian [21] in a formally covariant way. The specific model used here has been solved for the $q\bar{q}$ system in [17,18] and applied to a wide range of phenomena [19,29] including the heavy quark sector [9,20]. Details of the model may therefore be found in the references given in the Introduction. Here, I give a short survey and summarize some results.

Within the approximations given above the p_0 integration in the Bethe-Salpeter (BS) equation may be performed. The resulting Salpeter amplitude in the rest frame of the bound state with mass M is the given by

$$\Phi(\mathbf{p}) = \int \frac{dp^0}{(2\pi)} \chi_P(p^0, \mathbf{p})|_{P=(M, \mathbf{0})}, \quad (1)$$

where $\chi_P(p^0, \mathbf{p})$ is the full Bethe-Salpeter amplitude. Note that the relative momentum $p = (p_0, \mathbf{p})$ appearing in Eq. (1) may be written in a covariant fashion [17,18].

The resulting Salpeter equation is then given by

$$\begin{aligned} \Phi(\mathbf{p}) = & \int \frac{d^3 p'}{(2\pi)^3} \frac{\Lambda_1^-(\mathbf{p}) \gamma^0 [V(\mathbf{p}, \mathbf{p}') \Phi(\mathbf{p}')] \gamma^0 \Lambda_2^+(-\mathbf{p})}{M + \omega_1 + \omega_2} \\ & - \int \frac{d^3 p'}{(2\pi)^3} \frac{\Lambda_1^+(\mathbf{p}) \gamma^0 [V(\mathbf{p}, \mathbf{p}') \Phi(\mathbf{p}')] \gamma^0 \Lambda_2^-(-\mathbf{p})}{M - \omega_1 - \omega_2}. \end{aligned} \quad (2)$$

Here $\omega_i = \sqrt{\mathbf{p}^2 + m_i^2}$, and we introduce the energy projection operators $\Lambda_i^\pm(\mathbf{p}) = [\omega_i \pm H_i(\mathbf{p})]/(2\omega_i)$ in obvious notation, where $H_i(\mathbf{p}) = \gamma^0(\boldsymbol{\gamma} \cdot \mathbf{p} + m_i)$ is the standard Dirac Hamiltonian (for details see, e.g., Refs. [17,18]).

The dynamical input of the model is defined by a confinement plus one gluon exchange (OGE) kernel, $V = V_C + V_G$. Confinement is introduced as a mixture of a scalar- and a vector-type kernel in the following way:

$$[V_C(\mathbf{p}, \mathbf{p}') \Phi(\mathbf{p}')] = \mathcal{V}_C^S((\mathbf{p} - \mathbf{p}')^2) [\Phi(\mathbf{p}') - \gamma^0 \Phi(\mathbf{p}') \gamma^0]. \quad (3)$$

Because of the instantaneous approximation, it is possible to introduce the same spatial dependence (in the rest system of the meson) as used in the nonrelativistic case, viz., in coordinate space:

$$\mathcal{V}_C^F(r) = a_c + b_c r. \quad (4)$$

The mixture of a scalar and a vector spin structure has been introduced in order to give an improved description of the spin orbit splitting. Other mixtures have been advocated in the literature, and also an anomalous tensor-type confinement has been discussed; see, e.g., Ref. [7]. However, the consequences concerning, e.g., the mass spectrum or Regge behavior have not been studied yet.

For the OGE kernel, we chose the Coloumb gauge for the gluon propagator. This way it is possible to retain a covariant formulation within an instantaneous treatment of the Bethe-Salpeter equation, and it allows us to substitute q^2 by $-\mathbf{q}^2$. The OGE kernel then reads [23,24]

TABLE I. Parameters of the BS model.

$m_{u,d}$ [GeV]	m_s [GeV]	m_c [GeV]	m_b [GeV]	a_c [GeV]	b_c [GeV/fm]	r_0 [fm]	α_{sat}
0.200	0.440	1.738	5.110	-1.027	1.700	0.1	0.391

$$\begin{aligned} [V_G(\mathbf{p}, \mathbf{p}') \Phi(\mathbf{p}')] = & \mathcal{V}_G((\mathbf{p} - \mathbf{p}')^2) \\ & \times \left[\gamma^0 \Phi(\mathbf{p}') \gamma^0 - \frac{1}{2} [\boldsymbol{\gamma} \Phi(\mathbf{p}') \boldsymbol{\gamma} \right. \\ & \left. + (\boldsymbol{\gamma} \hat{\mathbf{x}}) \Phi(\mathbf{p}') (\boldsymbol{\gamma} \hat{\mathbf{x}}) \right], \end{aligned} \quad (5)$$

with the operator $\hat{\mathbf{x}} = \mathbf{x}/|\mathbf{x}|$, and

$$\mathcal{V}_G(\mathbf{q}^2) = \pi \frac{4}{3} \frac{\alpha_s(\mathbf{q}^2)}{\mathbf{q}^2}, \quad (6)$$

where $\alpha_s(q^2)$ is introduced as a ‘‘running’’ coupling as discussed in Refs. [9,17,18].

To solve the Salpeter equation numerically, Eq. (2) is rewritten as an eigenvalue problem (RPA equations); see, e.g., Refs. [17,21]. This way it is possible to utilize the variational principle to find the respective bound states. To this end the Salpeter amplitude Φ is expanded into a reasonably large number of basis states used as a test function. As a suitable choice of basis states we have taken Laguerre polynomials and found that about ten basis states lead to sufficient accuracy; see also Refs. [17,18].

For completeness, the parameters of the model given in Ref. [9] are shown in Table I. These are the quark masses, the offset a_c , and slope b_c of the confinement interaction, Eq. (4), and the saturation value $\alpha_{sat} = \alpha_s(\mathbf{q}^2 \rightarrow 0)$. They are determined to give a good overall description of the meson mass spectrum (heavy and light mesons as well as charmonium and bottomonium) [9,17–20,29].

B. Current matrix elements

Semileptonic decays are treated in a current-current approximation. For a transition $b \rightarrow c$ the Lagrangian is given by

$$\mathcal{L}_{cb} = \frac{G_F}{\sqrt{2}} V_{cb} h_{cb}^\mu j_\mu, \quad (7)$$

with the CKM matrix element V_{cb} and the Fermi constant G_F . The leptonic j_μ and hadronic currents h_{cb}^μ are defined by

$$j_\mu = \bar{l} \gamma_\mu (1 - \gamma_5) \nu_l, \quad (8)$$

$$h_{cb}^\mu = \bar{c} \gamma^\mu (1 - \gamma_5) b. \quad (9)$$

The relevant transition amplitudes

$$\langle D^{(*)} | \bar{c} \gamma^\mu (1 - \gamma_5) b | B \rangle \quad (10)$$

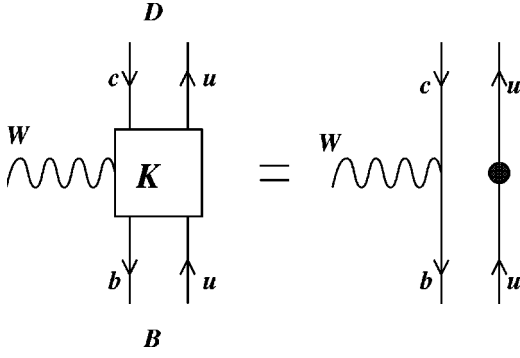


FIG. 1. Pictorial demonstration of the irreducible kernel of the full Mandelstam current for the $B \rightarrow D^{(*)}$ transition [left-hand side (LHS)] and its relativistic impulse approximation (RHS) used in Eq. (11). The solid circle denotes the inverse quark propagator.

for $B \rightarrow D$ and $B \rightarrow D^*$ of the hadronic current can be decomposed due to the Lorentz structure of the current, thus introducing form factors. A standard representation of the form factors is given in terms of $F_0(q^2)$, $F_1(q^2)$ [or $f_+(q^2)$, $f_-(q^2)$] for $0^- \rightarrow 0^-$ transitions, and $V(q^2)$, $A_0(q^2)$, $A_1(q^2)$, $A_2(q^2)$ for $0^- \rightarrow 1^-$ transitions [30]. The exact definitions and further references have been given, e.g., in Ref. [33]. Note that $m_l^2 \leq q^2 \leq q_{max}^2 = (m_B - m_{D^{(*)}})^2$ due to kinematical reasons. Helicity amplitudes H_\pm and H_0 in terms of the above form factors have been given by Körner and Schuler in a series of papers [30] and are compiled by the Particle Data Group [1]. Using the helicity amplitudes the formulas for the decay spectrum used here are given in Ref. [30] and will not be repeated here. The respective decay rates into specific helicity states Γ_\pm , Γ_0 are also given in the literature; see, e.g., Ref. [1].

To determine the form factors from the model, we follow the general prescription by Mandelstam [27]; see, e.g., Ref. [34] for a textbook treatment. The lowest order contribution (relativistic impulse approximation) to the current (sometimes referred to as a triangle graph) is given in Fig. 1, and written as (consider, e.g., the antiquark current, flavor indices suppressed)

$$\begin{aligned} \langle D^*, P_{D^*} | h_{cb}^\mu(0) | B, P_B \rangle \\ = - \int \frac{d^4 p}{(2\pi)^4} \text{tr} \{ \bar{\Gamma}_{P_{D^*}}(p - q/2) S_q^F(P_B/2 + p - q) \\ \times \gamma^\mu (1 - \gamma_5) S_q^F(P_B/2 + p) \Gamma_{P_B}(p) S_q^F(-P_B/2 + p) \}, \end{aligned} \quad (11)$$

where p and p' denote the relative momenta of the incoming and outgoing $q\bar{q}$ pair, and $q = P_{D^*} - P_B$ is the momentum transfer. The quark Feynman propagator is denoted by S_q^F . The Dirac coupling to pointlike particles is consistent with the use of free quark propagators. In Eq. (11) the amputated Bethe-Salpeter amplitude or vertex function $\Gamma_P(p)$ is given by

$$\Gamma_P(p) := [S_q^F(p_q)]^{-1} \chi_P(p) [S_q^F(-p_{\bar{q}})]^{-1}. \quad (12)$$

It may be computed in the rest frame from the equal time amplitude $\Phi(\mathbf{p})$ using the Bethe-Salpeter equation

$$\Gamma_P(p)|_{P=(M,0)} \equiv \Gamma(\mathbf{p}) = -i \int \frac{d^3 p'}{(2\pi)^4} [V(\mathbf{p}, \mathbf{p}') \Phi(\mathbf{p}')]. \quad (13)$$

Finally, using the Lorentz transformation properties of the field operators that define the Bethe-Salpeter amplitude [34], we can calculate the Bethe-Salpeter amplitude in any reference frame via

$$\chi_P(p) = S_{\Lambda_P} \chi_{(M,0)}(\Lambda_P^{-1} p) S_{\Lambda_P}^{-1}, \quad (14)$$

where Λ_P is the pure Lorentz boost and S_{Λ_P} the corresponding transformation matrix for Dirac spinors.

Because of the reconstruction of the full Bethe-Salpeter amplitude sketched above, the transition matrix element, Eq. (11), is manifestly covariant.

C. Form factors

The analysis of experimental data on heavy-to-heavy transitions now widely uses the notion of heavy quark expansion [1]. Following Ref. [31] we for one introduce the ratios $R_1(\omega)$ and $R_2(\omega)$:

$$R_1(\omega) \equiv \left[1 - \frac{q^2}{(m_B + m_{D^*})^2} \right] \frac{V(q^2)}{A_1(q^2)}, \quad (15)$$

$$R_2(\omega) \equiv \left[1 - \frac{q^2}{(m_B + m_{D^*})^2} \right] \frac{A_2(q^2)}{A_1(q^2)}, \quad (16)$$

where $\omega = (m_B^2 + m_{D^*}^2 - q^2)/(2m_B m_{D^*})$.

For $B \rightarrow D^* e \nu$ decays the standard form factors may then be related to the ones used for the heavy quark expansion by [31]

$$A_1(q^2) = \kappa_{BD^*} \left[1 - \frac{q^2}{(m_B + m_{D^*})^2} \right] h_{A_1}(\omega), \quad (17)$$

$$A_2(q^2) = \kappa_{BD^*} R_2(\omega) h_{A_1}(\omega), \quad (18)$$

$$V(q^2) = \kappa_{BD^*} R_1(\omega) h_{A_1}(\omega), \quad (19)$$

where $\kappa_{BD^*} = (m_B + m_{D^*})/(2\sqrt{m_B m_{D^*}})$. In the heavy quark mass limit ($m_{c,b} \rightarrow \infty$),

$$h_{A_1}(\omega) \rightarrow \xi(\omega), \quad (20)$$

$$R_{1,2}(\omega) \rightarrow 1, \quad (21)$$

where $\xi(\omega)$ is a universal function known as the Isgur-Wise function [2].

For the case $B \rightarrow D e \nu$ the standard form factors are related to the heavy quark form factors via [31]

$$f_+(q^2) = \kappa_{BD}^+ h_+(\omega) - \kappa_{BD}^- h_-(\omega), \quad (22)$$

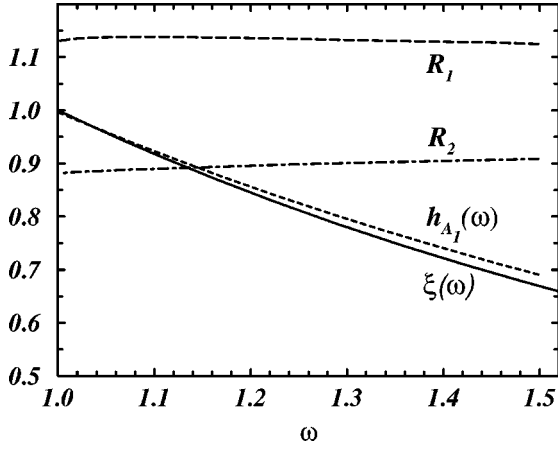


FIG. 2. Form factors $R_1(\omega)$ (long-dashed line), $R_2(\omega)$ (dash-dotted line), and $h_{A_1}(\omega)$ for the $B \rightarrow D^*$ transition as a function of ω . The Isgur-Wise function $\xi(\omega)$ of the heavy quark mass limit is shown as a solid line. Radiative corrections are not included here.

$$f_-(q^2) = \kappa_{BD}^+ h_-(\omega) - \kappa_{BD}^- h_+(\omega), \quad (23)$$

where $\kappa_{BD}^\pm = (m_B \pm m_D) / (2\sqrt{m_B m_D})$. In the heavy quark mass limit $h_+(\omega) \rightarrow \xi(\omega)$ and $h_-(\omega) \rightarrow 0$.

In the model approach used here the heavy quark mass limit has been performed numerically by multiplying $m_{c,b}$ with a large factor and keeping all other parameters as given in Table I. To evaluate the transition matrix elements, Eq. (11), the meson amplitudes are then calculated by diagonalizing the eigenvalue problem with the large quark masses. Because of numerical reasons, the heavy quark masses cannot be chosen too large. The function resulting from this numerical limiting procedure is then defined to be the Isgur Wise function $\tilde{\xi}(\omega)$ of the Bethe-Salpeter model, where $\tilde{\xi}(1) = 1.00$ within 0.1%. This function is shown as a solid line in Fig. 2. Note that at this stage $\tilde{\xi}$ does not include radiative corrections that will be given below. In the same fashion the ratios R_1 and R_2 tend to unity within less than 0.1% when numerically increasing the heavy quark masses.

For finite masses the experimental ratios $R_{1,2}$, assuming constant values, have recently been extracted by CLEO [3]. The latest values are [32]

$$R_1 = 1.24 \pm 0.26 \pm 0.12, \quad (24)$$

$$R_2 = 0.72 \pm 0.18 \pm 0.07, \quad (25)$$

which have to be contrasted to the long-dashed (R_1) and dash-dotted (R_2) curve shown in Fig. 2. The model ratios vary slowly by roughly 10% over the whole ω range, which is smaller than the experimental error.

III. RESULTS

Utilizing the Bethe-Salpeter model to describe mesons as $q\bar{q}$ states the exclusive decay spectra for $B \rightarrow D^* e \nu$ and $B \rightarrow D e \nu$ have been calculated and compared to the experimental data. Earlier the CKM matrix element $|V_{cb}|$ was determined by a least squares fit to the whole spectrum of

$B \rightarrow D^* e \nu$ [9]. We have now redone this analysis on the basis of the improved data and also included the recently measured $B \rightarrow D e \nu$ decay spectrum. In addition, we present a new analysis for this model approach at zero recoil of $B \rightarrow D^* e \nu$ that is commonly used for heavy-to-heavy transitions to extract $|V_{cb}|$. This enables us to compare the difference between the energy-dependent and zero-recoil analyses quantitatively, at least for the Bethe-Salpeter model discussed here and the nonrelativistic approach given earlier [33].

A. $B \rightarrow D^* e \nu$ decay

We now turn to the extraction the CKM matrix element $|V_{cb}|$. The differential decay rate for $B \rightarrow D^* e \nu$ is given by [1,35]

$$\begin{aligned} \frac{d\Gamma_{D^*}}{d\omega} = & \frac{G_F^2}{48\pi^3} m_{D^*}^3 (m_B - m_{D^*})^2 \sqrt{\omega - 1} \\ & \times (\omega + 1)^3 |V_{cb}|^2 \mathcal{F}_{D^*}^2(\omega) \\ & \times \left[1 + \frac{4\omega}{\omega + 1} \frac{m_B^2 + m_{D^*}^2 - 2\omega m_B m_{D^*}}{(m_B - m_{D^*})^2} \right]. \quad (26) \end{aligned}$$

The formula is written in a way that $\mathcal{F}_{D^*}(\omega)$ reduces to $\mathcal{F}_{D^*}(\omega) \rightarrow \eta_A \tilde{\xi}(\omega) = \xi(\omega)$ in the heavy quark mass limit, where η_A denotes the radiative corrections [31,36]. For finite masses the function $\mathcal{F}_{D^*}(\omega)$ contains all the symmetry breaking effects.

Experiments are given in a way that all well known factors are divided out in the decay rate and only $|V_{cb}| \mathcal{F}_{D^*}(\omega)$ is left over. The corresponding data points of a recent CLEO measurement are shown in Fig. 3. The result is particularly smooth and may be fitted by a linear curve. The fit to the data done by the CLEO Collaboration is also shown in Fig. 3 as a dash-dotted line. Other lines reflect the model results utilizing different assumptions. The solid line is calculated using the exact formula for the decay rate as given, e.g., in [1,30] (i.e., with $R_{1,2}$ ω dependent) divided by the same factor as the experiments are. The CKM matrix element $|V_{cb}|$ is then determined by a least squares fit to all data points. Radiative corrections have been included in the dominant form factor $h_{A_1}(\omega)$, expressed as an overall factor η_A [31]. Unlike earlier estimates that imply a correction of approximately 1% [31] (i.e., smaller than the model uncertainty and therefore neglected in the earlier analysis [9]) a recent two-loop calculation leads to a substantial value of $\eta_A = 0.960 \pm 0.007$ [36], which has to be included in the analysis. The result is $|V_{cb}| = 0.0339 \pm 0.0010$. To see the model dependence of the different analyses used in this context we now take $\mathcal{F}_{D^*}(\omega) = \eta_A h_{A_1}(\omega)$, R_1 and R_2 constant, i.e., $R_1(1)$, $R_2(1)$, and this CKM matrix element that leads to the long-dashed line shown in Fig. 3. It is obvious that the curve slightly deviates from the solid one that includes the ω dependence of R_1 and R_2 . Using the same ω dependence for $\mathcal{F}(\omega)$, however, the value of $|V_{cb}| \mathcal{F}_{D^*}(\omega=1)$ from the CLEO fit leads to the

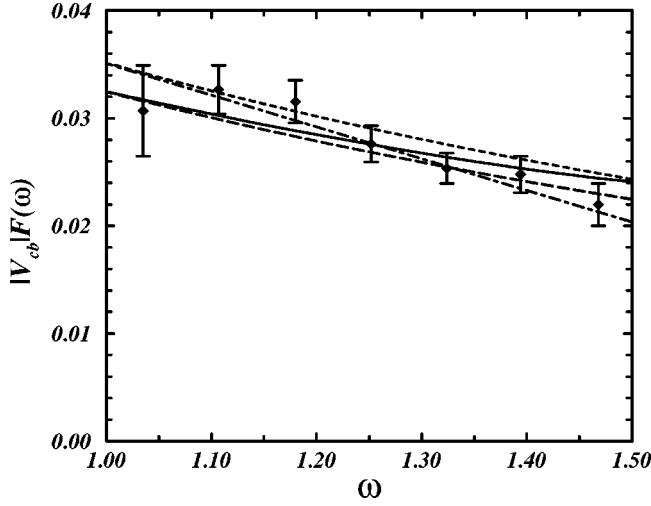


FIG. 3. $|V_{cb}|\mathcal{F}(\omega)$ as a function of ω for $B \rightarrow D^* e \nu$ decays. Data points are from the CLEO Collaboration, and the dash-dotted line shows their linear fit (with $c=0$) to the data. The model result using $|V_{cb}|$ of Eq. (31) is displayed as a solid line. The long-dashed line shows the model result using the same value for $|V_{cb}|\mathcal{F}$ at $\omega=1$ but constant $R_{1,2}$ (as used in the zero-recoil analysis). The dashed line uses the value of $|V_{cb}|$ as provided by the CLEO Collaboration and $R_{1,2}$ constant (i.e., zero-recoil method) for comparison.

short-dashed curve. The resulting CKM matrix element is obviously larger by $\approx 8\%$.

The function $\mathcal{F}_{D^*}(\omega)$ that leads to Fig. 3 can be approximated by a quadratic fit to

$$\mathcal{F}_{D^*}^{(2)}(\omega) = \mathcal{F}_{D^*}(1)[1 - \rho_{A_1}^2(\omega - 1) + c(\omega - 1)^2], \quad (27)$$

with the parameters $\rho_{A_1}^2$ and c . The slope of $\mathcal{F}_{D^*}(\omega)$ extracted by CLEO [3] assuming a linear dependence on ω ($c=0$) is $\rho_{A_1}^2 = 0.84 \pm 0.13 \pm 0.08$, and is shown as a dash-dotted line in Fig. 3. The respective parameters for the quadratic fit of the curve discussed are shown in Table II.

Within the notion of the heavy quark effective theory the form factor $\mathcal{F}_{D^*}(\omega=1)$ can be expanded into orders of $\Lambda_{QCD}/m_{c,b}$. Since symmetry breaking effects in semileptonic decays are of second order only [37], lowest order terms are usually written as

$$\mathcal{F}_{D^*}(\omega=1) = \eta_A(1 + \delta_{1/m^2}), \quad (28)$$

TABLE II. Parameters for a quadratic fit to the CLEO data and the BS model. The first line is in the heavy quark mass limit, other lines for physical masses.

$\rho_{A_1}^2$	c	Model
0.83	0.34	for $\xi_{BS}(\omega)$
0.76	0.30	for $h_{A_1}(\omega)$
0.69	0.34	for $\mathcal{F}(\omega)$
$0.92 \pm 0.64 \pm 0.40$	$0.15 \pm 1.24 \pm 0.90$	CLEO data

where δ_{1/m^2} has to be determined. Corrections vary from $-\delta_{1/m^2} = (3 \pm 2)\%$ [38,39] to $-\delta_{1/m^2} = (5.5 \pm 2.5)\%$ [40]. A recent discussion and appreciation of the different approaches is given by Martinelli [41]. The relativistic model discussed here leads to a value of $-\delta_{1/m^2} = 0.5\%$.

The values for $\mathcal{F}_{D^*}(\omega=1)|V_{cb}|$ that have been extracted by different experiments are quite consistent and lead to an overall fit of [41,32]

$$\mathcal{F}_{D^*}(\omega=1)|V_{cb}| = 0.0343 \pm 0.0015 \quad (29)$$

for the empirical slope parameter given in the last line of Table II. Using this value and the radiative corrections given above we extract the CKM matrix element $|V_{cb}|$ for the relativistic Bethe-Salpeter model to be

$$|V_{cb}| = 0.0360 \pm 0.0016 \quad \text{zero recoil}, \quad (30)$$

$$|V_{cb}| = 0.0339 \pm 0.0010 \quad \text{full spectrum}. \quad (31)$$

This is the main result that shows the potential model dependence of the zero-recoil method that adds to the statistical uncertainty. A similar renewed analysis for the nonrelativistic model given before [33] now leads to $|V_{cb}| = 0.037 \pm 0.002$, which is larger by 7% compared to the spectrum-dependent analysis. For definiteness a B lifetime of $\tau_B = 1.56$ ps has been used throughout the analysis to extract $|V_{cb}|$.

The values for $|V_{cb}|$ extracted here from exclusive decays are compatible with results found by other models, e.g., ranging from $|V_{cb}| = 0.034 \pm 0.003$ to $|V_{cb}| = 0.037 \pm 0.004$ using a dispersion approach [42], light front quark models [43], the nonrelativistic model [5], and simple form factor parametrizations [4,30]. The values extracted from inclusive decays appear to be also compatible with a slight preference for higher values ranging from $|V_{cb}| = 0.038 \pm 0.003$ to $|V_{cb}| = 0.043 \pm 0.003$ for five different models [44].

B. $B \rightarrow D e \nu$ decay

The differential decay rate for the $B \rightarrow D e \nu$ is given by [35]

$$\frac{d\Gamma}{d\omega} = \frac{G_F^2}{48\pi^3} m_D^3 (m_B + m_{D^*})^2 (\omega - 1)^{3/2} |V_{cb}|^2 \mathcal{F}_D^2(\omega), \quad (32)$$

where again $\mathcal{F}_D(\omega)$ reduces to the Isgur-Wise function in the heavy quark mass limit. Recent experimental data for the relevant part of the spectrum $|V_{cb}|\mathcal{F}_D(\omega)$ are shown in Fig. 4. The linear fit to the data given by the CLEO Collaboration is also shown (as a dash-dotted line). The model results utilizing the full spectrum-dependent analysis lead to the solid line in Fig. 4. For comparison the result of the zero-recoil method utilized in the previous paragraph is also shown. The radiative corrections have been assumed to be in the same order as in the $B \rightarrow D^* e \nu$ transition. Obviously the model is capable of providing a good description of the experimental data.

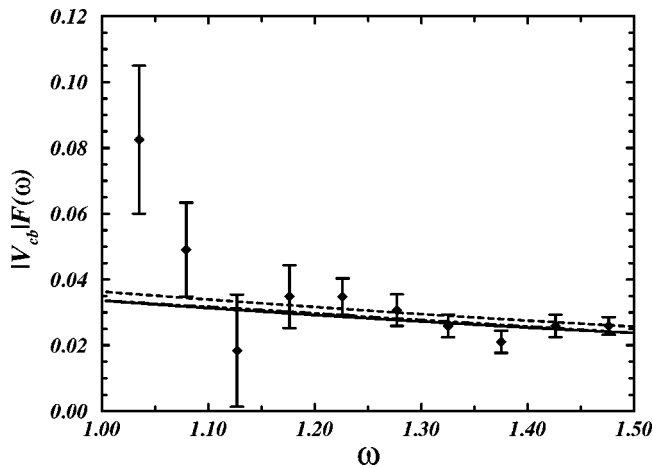


FIG. 4. $|V_{cb}|\mathcal{F}(\omega)$ as a function of ω for $B \rightarrow D e \nu$ decays. Data points are from the CLEO Collaboration, and the dash-dotted line shows their linear fit (with $c=0$) to the data. The model result using $|V_{cb}|$ of Eq. (31) is displayed as a solid line.

IV. SUMMARY AND CONCLUSION

We have analyzed the exclusive decay rates of $B \rightarrow D^* e \nu$ and $B \rightarrow D e \nu$ within a relativistic constituent quark model. The interaction kernel has been taken to be instantaneous. This way the Bethe-Salpeter equation reduces to a Salpeter equation as given in Eq. (2). The interaction consists of a one-gluon exchange evaluated in the Coulomb gauge and a linear confinement given in coordinate space. The model parameters have been fixed to describe the mass spectrum of all observed mesons (not only heavy mesons) in a satisfactory manner [17–20]. The interaction current to describe the weak decay process has been introduced via the Mandelstam formalism. To this end the (instantaneous) am-

plitude has been reconstructed using the Lorentz transformation properties of the field operators.

The only parameter left to describe the exclusive decay spectra is the CKM matrix element $|V_{cb}|$. For $B \rightarrow D^* e \nu$ two methods have been compared. One uses the complete spectrum, viz., the functional dependence of \mathcal{F}_{D^*} , emerging from the quark model. The CKM matrix element is then fixed by a least squares fit. The other analysis utilizes the “zero-recoil” method used in the context of heavy quark expansion. Here only the empirical value of $|V_{cb}|\mathcal{F}_{D^*}(1)$ is used that is gained from an extrapolation of the experimental data (e.g., by a linear fit) to the zero-recoil point $\omega=1$ and R_1, R_2 assumed constant. The CKM matrix element $|V_{cb}|$ is then extracted using a singular value of the model at $\mathcal{F}_{D^*}(1)$. Clearly, this method is not consistent with the underlying model, but widely used to extract $|V_{cb}|$ from the zero-recoil point. Comparing the full model result to the zero-recoil result leads to different values for the CKM matrix elements $|V_{cb}|$ by approximately 8%. In view of this result it seems obvious that this kind of model uncertainty stemming from the different treatment of the ω dependence of the spectrum may show up in the determination of $|V_{cb}|$ in addition to the statistical error. This result may also be relevant for other more “model-independent” analyses.

For comparison the $B \rightarrow D e \nu$ decay has been calculated for the different assumptions and also leads to a good overall description of the experimental spectrum.

ACKNOWLEDGMENTS

I would like to thank G. Zöller for his previous contributions to this work. I am grateful to D.I. Melikhov for valuable comments on the manuscript and discussions. Also I would like to thank T. Mannel for his interest and R. Faustov for discussions on some general issues.

-
- [1] Particle Data Group, R. M. Barnett *et al.*, Phys. Rev. D **54**, 1 (1996); 1997 off-year partial update for the 1998 edition available on the PDG WWW pages (URL: <http://pdg.lbl.gov/>).
- [2] N. Isgur and M. B. Wise, Phys. Lett. B **232**, 113 (1989); **237**, 527 (1990).
- [3] CLEO Collaboration, S. Sanghera *et al.*, Phys. Rev. D **47**, 791 (1993); B. Barish *et al.*, *ibid.* **51**, 1014 (1995); J. E. Dubosq *et al.*, Phys. Rev. Lett. **76**, 3898 (1996).
- [4] M. Wirbel, B. Stech, and M. Bauer, Z. Phys. C **29**, 637 (1985).
- [5] N. Isgur, D. Scora, B. Grinstein, and M. B. Wise, Phys. Rev. D **39**, 799 (1989).
- [6] W. Jaus, Phys. Rev. D **41**, 3394 (1990); **53**, 1349 (1996).
- [7] V. O. Galkin, A. Yu. Mishurov, and R. N. Faustov, Sov. J. Nucl. Phys. **55**, 1207 (1992); R. N. Faustov, V. O. Galkin, and A. Yu. Mishurov, Phys. Rev. D **53**, 1391 (1996); R. N. Faustov, V. O. Galkin, and A. Yu. Mishurov, Phys. Lett. B **356**, 516 (1995); **367**, 391E (1996); R. N. Faustov and V. O. Galkin, Z. Phys. C **66**, 119 (1995).
- [8] D. Scora and N. Isgur, Phys. Rev. D **52**, 2783 (1995).
- [9] G. Zöller, S. Hainzl, C. R. Münz, and M. Beyer, Z. Phys. C **68**, 103 (1995); G. Zöller, diploma thesis, Bonn University, 1994.
- [10] I. L. Grach, I. M. Narodetskii, and S. Simula, Phys. Lett. B **385**, 317 (1996).
- [11] D. Melikhov, Phys. Lett. B **394**, 385 (1997); **380**, 363 (1996); Phys. Rev. D **53**, 2460 (1996).
- [12] H.-Y. Cheng, C.-Y. Cheung, and C.-W. Hwang, Phys. Rev. D **55**, 1559 (1997).
- [13] A. Le Yaouanc, in *Proceedings of the IVth International Workshop on Progress in Heavy Quark Physics*, Rostock, 1997, edited by M. Beyer, T. Mannel, and H. Schröder (Rostock University Press, Rostock, 1998), p. 129.
- [14] V. Braun, in *Proceedings of the IVth International Workshop on Progress in Heavy Quark Physics* [13], p. 105.
- [15] C. Sachrajda, *Heavy Flavours*, edited by A. J. Buras and M. Lindner (World Scientific, Singapore, in press), hep-lat/9710057.
- [16] B. Stech, Z. Phys. C **75**, 245 (1997).
- [17] J. Resag, C. R. Münz, B. C. Metsch, and H. R. Petry, Nucl. Phys. **A578**, 397 (1994).
- [18] C. R. Münz, J. Resag, B. C. Metsch, and H. R. Petry, Nucl. Phys. **A578**, 418 (1994).

- [19] C. R. Münz, J. Resag, B. C. Metsch, and H. R. Petry, Phys. Rev. C **52**, 2110 (1995).
- [20] J. Resag and C. R. Münz, Nucl. Phys. **A590**, 735 (1995).
- [21] J. F. Lagaë, Phys. Rev. D **45**, 305 (1992); **45**, 317 (1992).
- [22] H. Hersbach, Phys. Rev. A **46**, 3657 (1992); Phys. Rev. D **47**, 3027 (1993).
- [23] E. Hummel and J. Tjon, Phys. Rev. C **42**, 423 (1990); J. A. Tjon, *ibid.* **41**, 472 (1990); P. C. Tiemeijer and J. A. Tjon, Phys. Lett. B **277**, 38 (1992); Phys. Rev. C **48**, 494 (1993); **48**, 896 (1994).
- [24] T. Murota, Prog. Theor. Phys. **69**, 181 (1983); **69**, 1498 (1983).
- [25] Yu. L. Kalinovsky and C. Weiss, Z. Phys. C **63**, 275 (1994).
- [26] E. E. Salpeter and H. A. Bethe, Phys. Rev. **84**, 1232 (1951).
- [27] S. Mandelstam, Proc. R. Soc. London **A233**, 248 (1955).
- [28] A. Bilal and P. Schuck, Phys. Rev. D **31**, 2045 (1985).
- [29] E. Klempt, B. C. Metsch, C. R. Münz, and H. R. Petry, Phys. Lett. B **361**, 160 (1995); W. I. Giersche and C. R. Münz, Phys. Rev. C **53**, 2554 (1996); C. R. Münz, Nucl. Phys. **A609**, 364 (1996).
- [30] J. G. Körner and G. A. Schuler, Z. Phys. C **38**, 511 (1988); **41**, 690(E) (1989); **46**, 93 (1990).
- [31] M. Neubert, Phys. Rep. **245**, 259 (1994).
- [32] CLEO Collaboration, in *Proceedings of the IVth International Workshop on Progress in Heavy Quark Physics* [13], p. 67.
- [33] S. Resag and M. Beyer, Z. Phys. C **63**, 121 (1994).
- [34] D. Lurie, *Particles and Fields* (Interscience Publishers, New York, 1968).
- [35] M. Neubert, Phys. Lett. B **264**, 455 (1991).
- [36] A. Czarnecki, Phys. Rev. Lett. **76**, 4124 (1996).
- [37] M. E. Luke, Phys. Lett. B **252**, 447 (1990).
- [38] A. F. Falk and M. Neubert, Phys. Rev. D **47**, 2965 (1993); **47**, 2982 (1993).
- [39] T. Mannel, Phys. Rev. D **50**, 428 (1994).
- [40] M. A. Shifman, N. G. Uraltsev, and A. Vainshtein, Phys. Rev. D **51**, 2217 (1995).
- [41] G. Martinelli, Nucl. Instrum. Methods Phys. Res. A **384**, 241 (1996).
- [42] D. I. Melikhov, Phys. Lett. B **394**, 385 (1997).
- [43] N. B. Demchuk, P. Yu. Kulikov, I. M. Narodetskii, and P. J. O'Donnell, Phys. At. Nucl. **60**, 1292 (1997).
- [44] I. Narodetskii, in *Proceedings of the IVth International Workshop on Progress in Heavy Quark Physics* [13], p. 181.